



Instrument Science Report NICMOS 2008-002

Improvements to Calnica

T. Dahlen, H. McLaughlin, V. Laidler, M. Regan, E. Bergeron, R. Jedrzejewski,
R. Bohlin, R. de Jong, A. Viana
June 04, 2008

ABSTRACT

This ISR describes a number of improvements to `calnica`, the STSDAS task that performs routine instrumental calibration of NICMOS raw images. We report two major and a number of minor updates to the code. The major updates consist of changes in the way the count rate is calculated from up-the-ramp fitting and changes in the cosmic rays rejection algorithm. All updates have been extensively tested and analysis shows improvement in the S/N of output images by 6-15% compared to the previous `calnica` version. A further improvement is that the error extension in the calibrated images now represents the true errors in a more consistent way compared to the old implementation of the software.

Introduction

The `calnica` task performs instrumental calibration of NICMOS data, including dark current subtraction, correction for detector non-linearity, flat-fielding, conversion to count rates, population of photometric keywords, and cosmic ray identification and rejection. `calnica` is available in the NICMOS package of STSDAS and is also used by STScI's On-the-fly Reprocessing (OTFR) when final calibrated images are requested from the archive.

In this report, we describe a number of updates made to the `calnica` task in order to improve its performance. The two major updates concern:

- The determination of count rate from up-the-ramp-fitting (page 2-4)
- Cosmic ray rejection (page 5)

Besides these, a number of minor updates are also described:

- Bias in the slope due to Poisson Noise (page 6-7)

- Maximum number of cosmic rays allowed (page 8)
- Curvature in up-the-ramp sampling (page 9)
- `_spt` file check (page 11)
- Spike rejection (page 11)
- Saturation in zeroth read (page 11)

To investigate the behavior of the new `calnica` version and to quantify the changes, we have compared results from the old and the new `calnica` versions for a large data set, including science as well as calibration data in both the low and high signal-to-noise (S/N) regime.

The new `calnica` Version 4.2 replaces the previous `calnica` Version 4.1.1 from 2002.

Determining the Count Rate from Up-the-Ramp Fitting

Background

A large majority of NICMOS observations use up-the-ramp (MULTIACCUM) sampling. In this mode, NICMOS reads out the detectors in a non-destructive way during an exposure. The count rate in each pixel is thereafter calculated by a least square fit to the accumulated counts at each read. This is equivalent to the slope of a straight line if plotting accumulated charge against time. Figure 1 shows fits to up-the-ramp sampling for the case of high S/N as well as low S/N (left and right panels, respectively). Red lines show the best-fitting slopes and the error-bars show typical read noise errors (smaller than symbols in left panel).

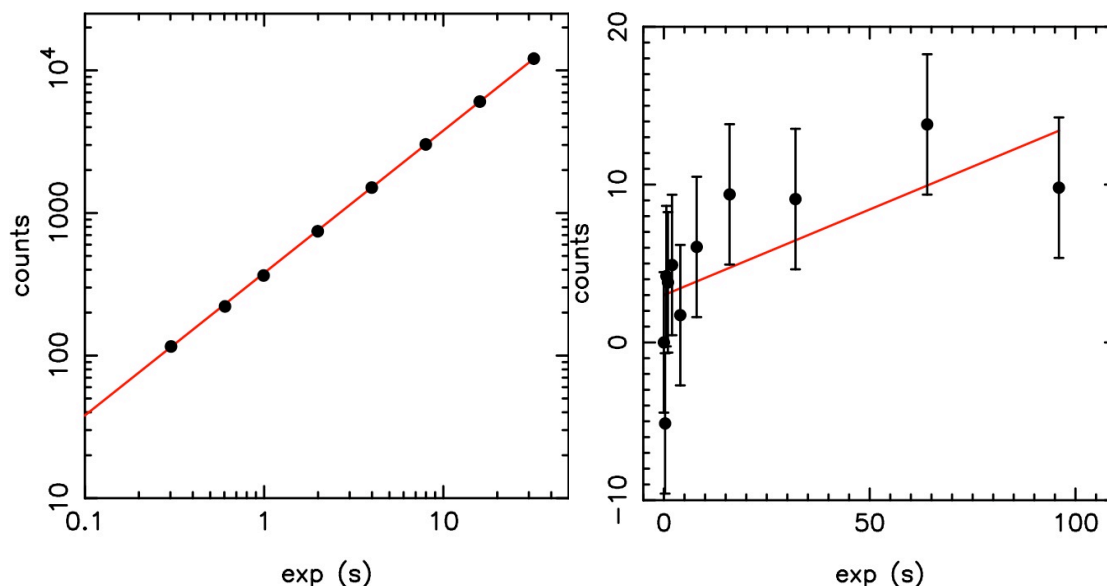


Figure 1: **Left panel shows an up-the-ramp sequence in the high S/N regime, while the right panel shows the case for low S/N. Red lines show the slope of the least-square fit to the samples. Error-bars show typical read noise errors. Note that the two panels have different scaling.**

Weighting the Up-the-Ramp Sampling

There are different ways of weighting each sample when calculating the least square fit to the up-the-ramp sampling. Fixsen et al. (2000) showed that the optimum way of doing this depends on whether you are in the read noise or Poisson noise dominated regime. For pure read noise, equal weighting of each sample gives the best result, while for Poisson noise only, using only the first and the last reads gives the best results. For any normal observational situation, the case will lie in between these. Fixsen et al. describe the optimum weighting to apply in these cases, a recipe that is applied here.

The following illustration of the optimum weighting is taken from Regan (2007), for a more detailed description we refer to that publication. In Figure 2, we show six cases with different S/N, reflecting whether we are in to read noise-dominated regime (low S/N) or Poisson dominated regime (high S/N). The six cases are described in Table 1. Each observation is assumed to consist of 200 reads. For the lowest S/N, the Figure shows that equal weights are applied to all reads (uppermost curve). Increasing the S/N leads to a weighting that becomes more and more dominated by the first and last reads. The equation used to determine the weight of the i^{th} read, W_i , is

$$W_i = (i - i_{\text{mid}})^P$$

where i_{mid} is the read number of the mid-point of the read sequence and P is the power that is determined by the signal-to-noise ratio of the last read, S. S is given by:

$$S = \frac{\text{Source_Electrons}}{\sqrt{\text{Source_Electrons} + \text{Read_noise}^2}}$$

The six different values of the P used in the Figure 1 correspond to the ranges of S/N shown in Table 1. Fixsen et al. showed that rather than solving for the optimum weight for each value of S, a small number of values of P recovers almost all of the gain in signal-to-noise.

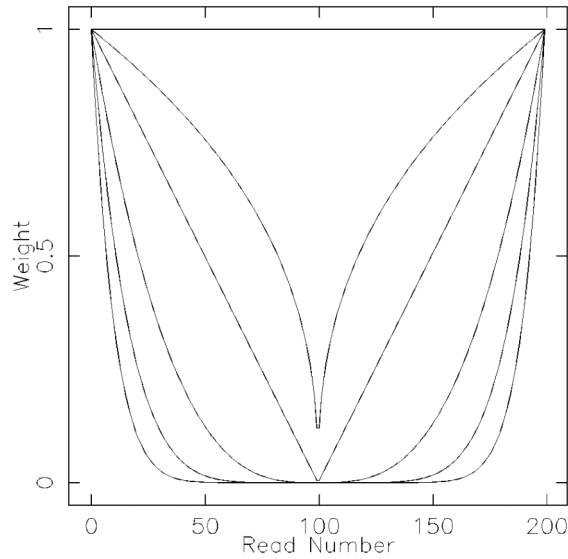


Figure 2: Optimum weighting scheme following Fixsen et al. (2000). For low S/N, equal weight is optimal, while for increasing S/N, the first and last reads become more dominating. Figure from Regan (2007).

Minimum S	Maximum S	P
0	5	0
5	10	.4
10	20	1
20	50	3
50	100	6
100		10

Table 1. The value of P, as defined above, as a function of the signal-to-noise of the last read, S. From Regan (2007).

For comparison, Figure 3 shows the weighting applied to the old version of *calnica* for the same six S/N regimes. For low S/N, equal weighting is applied similar to the optimum approach. With increased S/N, the difference becomes apparent. In the old scheme, the weight in latter reads decreases because this weight includes both read noise and Poisson noise. Since Poisson noise increases, the weight decreases. However, it is not correct to include the Poisson noise in this sense since there is no Poisson noise in a particular read. In each read, a finite number of electrons have been collected without any uncertainty in that actual number.

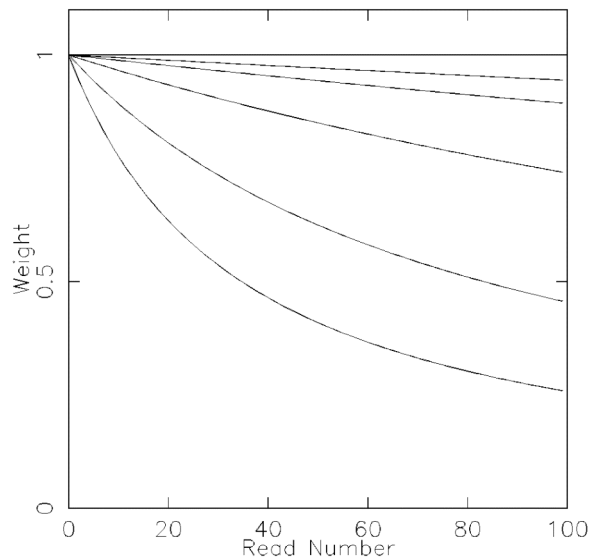


Figure 3. Weighting used in the previous version of *calnica*. The six curves corresponds to the same six values of P shown in Figure 2 and given in Table 1.

By using the optimum weighting instead of the weighting used by previous version of *calnica*, Fixen et al. (2000), show that the variance in the flux estimate based on up-the-ramp sampling decreases by up to 15%.

Cosmic Ray Rejection

One of the major advantages with multiple readout modes is that cosmic ray (hereafter CR) hits can be detected and corrected for. This is not the case for a single readout mode or a CCD, for which a pixel that is hit by a CR in a particular exposure cannot be used. In `calnica`, CRs are detected by first fitting the uncorrected slope of the up-the-ramp sequence to a straight line and thereafter looking for outliers of more than some predefined sigma value (default is a 4 sigma threshold). After a preliminary correction for any initially found CR, this procedure is iterated to look for multiple CRs in the sequence. Once a CR is flagged, the slope of the up-the-ramp sequence can be calculated using data from all reads, except the interval that was hit by the CR. However, the way this is done differs between the previous and new versions of `calnica`. We illustrate this in Figure 4, which shows the case of a CR hit during a MULTI ACCUM sequence. The black dots represent the counts in 20 readouts equally spaced in time. The CR causes a jump in the counts between read 10 and 11 (illustrated by stars). In the previous version, the counts after the CR hit was corrected by subtracting the difference between the post and pre CR hit reads. These “corrected” counts are shown with red symbols in Figure 4. Thereafter a straight line was fit over the whole up-the-ramp sequence. However, the difference between the pre and post CR reads will have an uncertainty that is $\sqrt{2} * (read - noise)$. When doing the subtraction, the uncertainty will bias all the post CR reads and therefore also bias the derivation of the slope. In Figure 4, we show the resulting slope according to the old method with the red line.

In the new version of `calnica`, the CR correction is done differently without adding the bias mentioned above. Instead of doing the subtraction and fitting over the whole sequence, the new method fits the slope independently for the pre CR reads and the post CR reads, shown in the figure as the solid black lines. Thereafter, the slopes are weighted together to derive a final slope, indicated by the dashed line (note that this is equivalent to doing a fit that simultaneously fits the jump and a single slope to all data). A maximum of three different slopes can be weighted together. With three or more CR hits, `calnica` will interpret this as curvature in the up-the-ramp sampling, as described below (page 9).

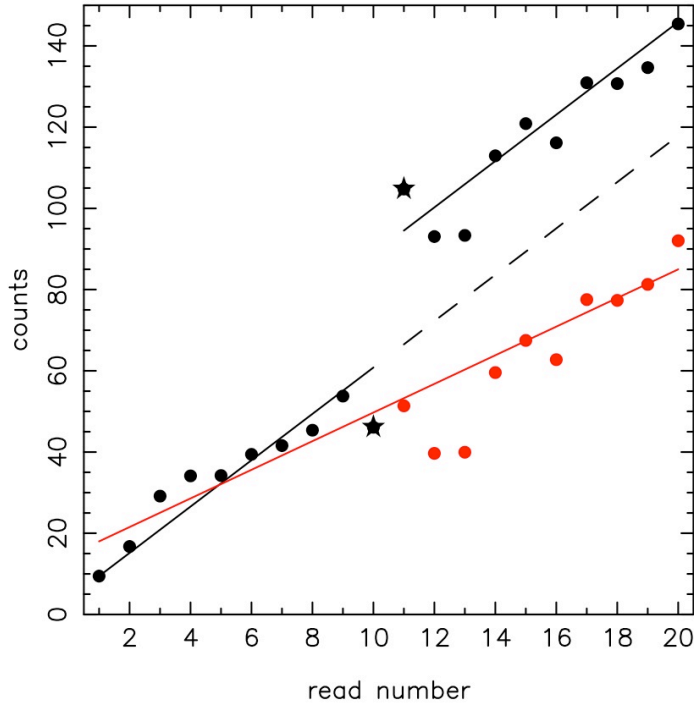


Figure 4: Black dots illustrates the counts in 20 MULTIACCUM readouts equally spaced in time, with a CR hit between reads 10 and 11 (shown with stars). Previous version of `calnica` corrected for the CR hit by subtracting the difference between the post and pre CR hit reads from all the post CR hit reads. This results in the red dots and a best fitting slope shown by the red solid line. The new version of `calnica` fits the pre and post CR sequences independently (shown by the two solid black lines) and thereafter weights these together to get the final slope (dashed line).

Minor Calnica Improvements

Bias in the Slope Due to Poisson Noise

The previous version of `calnica` included a Poisson term when calculating the weights used in the least square fit to the up-the-ramp slope. However, in cases of low count rates, this tends to bias the estimated slope towards zero. This is because each read will scatter around the true value of the accumulated counts with an rms given mainly by the read noise. Reads with a value below the true value will then be given a higher weight due to the smaller errors for these reads. The result will be a bias toward zero in the derived slope. Figure 5 shows the bias as a function of count rate for both the weighting used in the previous version of `calnica` and the new optimum weighting. The bias is more or less eliminated using the optimum weighting. In a normal case, however, this effect will not affect NICMOS observations using the old weighting since the broad-band background count rate is above the threshold (~ 1 electron/sec) under which the bias becomes significant.

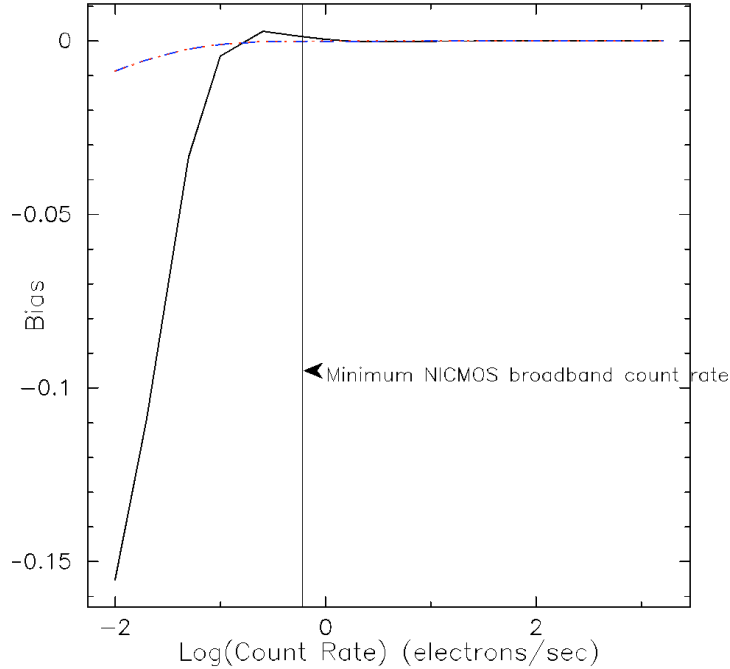


Figure 5. **Relative bias in the slope of the up-the-ramp fitting for different weightings. Solid line shows the case used by the previous version of `calnica`, while dashed-dotted line shows optimum weighting. Vertical line shows typical NICMOS broad-band background count rate.**

Bias in the Case of CR Hits

While the bias due to the inclusion of Poisson statistics in the low count rate regime will not affect the derived slope in any normal case, there will be a bias affecting the slope in cases with a CR hit. For example, if there is one CR hit during an exposure, then `calnica` will calculate two separate slopes for the pre and post CR sequences. These two slopes will have values that have some rms deviations from the true value of the slope. If Poisson statistics were included when weighting the slopes together, then the slope with the lowest value would be given a higher weight and thereby biasing pixels with CR hits toward zero.

In Figure 6, we show a histogram over the number of CR affected pixels with a given deviation of the slope away from the mean slope of the same pixel when it is not affected by a cosmic ray. The solid black line shows the previous version of `calnica` and the dashed blue line is the new version. The figure shows that there is a small bias shifting the results using the previous `calnica` to slightly more negative values (i.e., CR affected pixels were biased to lower slopes). However, the overall difference is not large between the two methods.

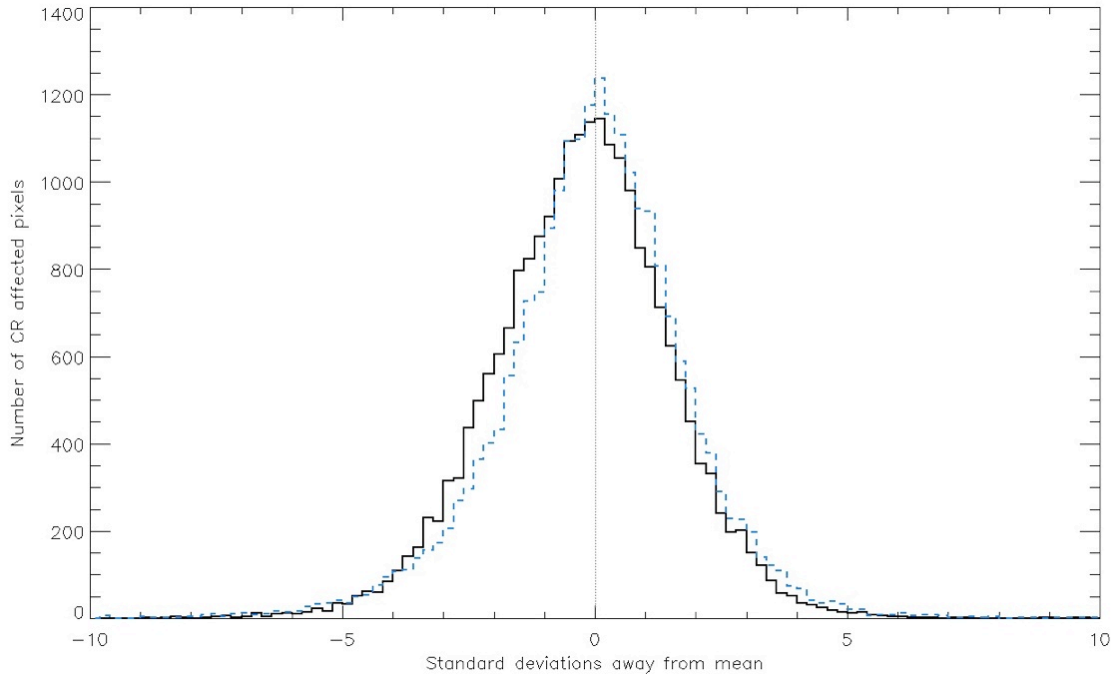


Figure 6: Histogram of CR affected pixels for a typical set of darks. The histogram shows the number of CR affected pixels with a given deviation of the slope away from the mean slope of the same pixel when it is not affected by a cosmic ray. The solid black line shows the previous version of `calnica` and the dashed blue line is the new version. There is a slight bias towards more negative values for the previous version of `calnica`. Overall, there is not a large difference in the two methods. Histogram is plotted for dark images using sequence STEP32/NSAMP=17.

Maximum CR Violation

The previous version of `calnica` was hard-coded to allow a maximum of ten CRs in each pixel during a single exposure. If this number was exceeded, the software would crash without notifying the reason for this. In any normal case, the statistical probability that ten CRs occur in one sequence is ‘non-existent’, so this should not be a problem. However, it turns out that in some particular cases, the up-the-ramp response of NICMOS is not linear, but instead shows a curvature. If the curvature is positive, then `calnica` may interpret the response as a series of CRs, which may lead to a crash. In the previous version of `calnica` that included the Poisson statistics in the weighting, this curvature went mostly unnoticed. With the new optimum weighting implemented, it turns out that under special circumstances, e.g., pixels near bright point sources, the curvature may cause the maximum number of CRs to be exceeded. As a safety precaution, `calnica` now checks that the maximum number of CRs is not exceeded. In the next section, we further describe how `calnica` deals with the pixels showing curvature in their response.

Curvature in the Up-the-Ramp Sampling

In particular cases, NICMOS shows a non-linear response that can have either a positive or a negative curvature. This effect occurs at “sharp” sources (bright point

sources, CRs). The particular program where this effect was discovered is PID 9750 (P.I: K Sahu, *The Galactic Bulge Deep Field: A Planetary Transit Survey and Very Deep Stellar Mass Function*).

Figure 7a+7b illustrates the curvature in the NIC2 response for pixels around a bright star in a crowded field (PID 9750). The left panel of Figure 7a shows a direct image of the star, while each line in Figure 7b shows the response of individual pixels relative to a straight-line fit for 8x8 pixels around the point source. Different curvatures are color-coded (blue=negative curvature, red=flat, yellow=positive curvature). Finally, the right panel of Figure 7a shows the spatial distribution of the pixels with different curvature with colors from Figure 7b.

When the detector reads out the signal in the fast read direction the detector seems to respond too slowly when going from a pixel with low counts to a high count pixel, resulting in a signal that is lower than expected (going from red to yellow in Figure 7a). When reading past the peak of the point source (green pixel), the detector instead overshoots, showing a curvature of the opposite sign (blue pixel).

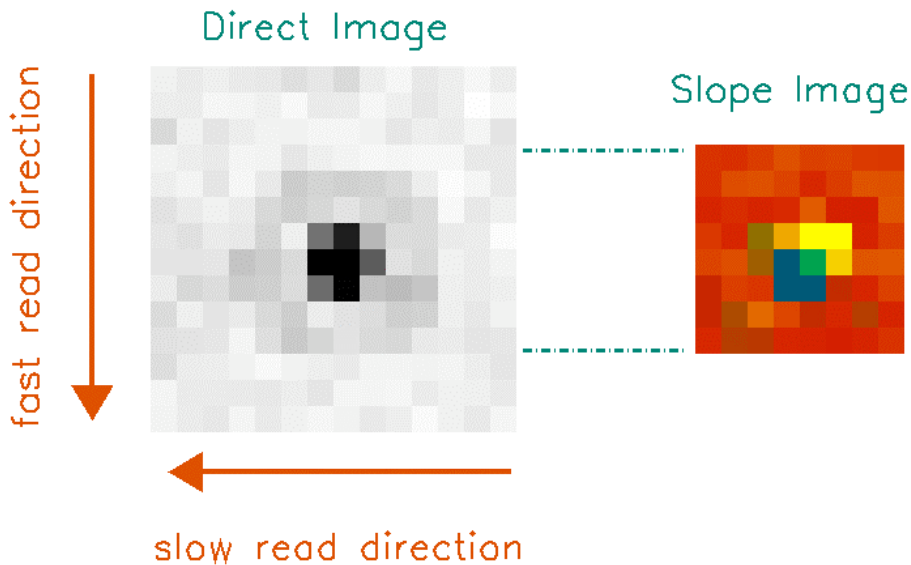


Figure 7a: Left panel shows a direct image of a bright point source while the right panel shows the curvature of the central 8x8 pixels around the source while color codes as in Figure 7b.

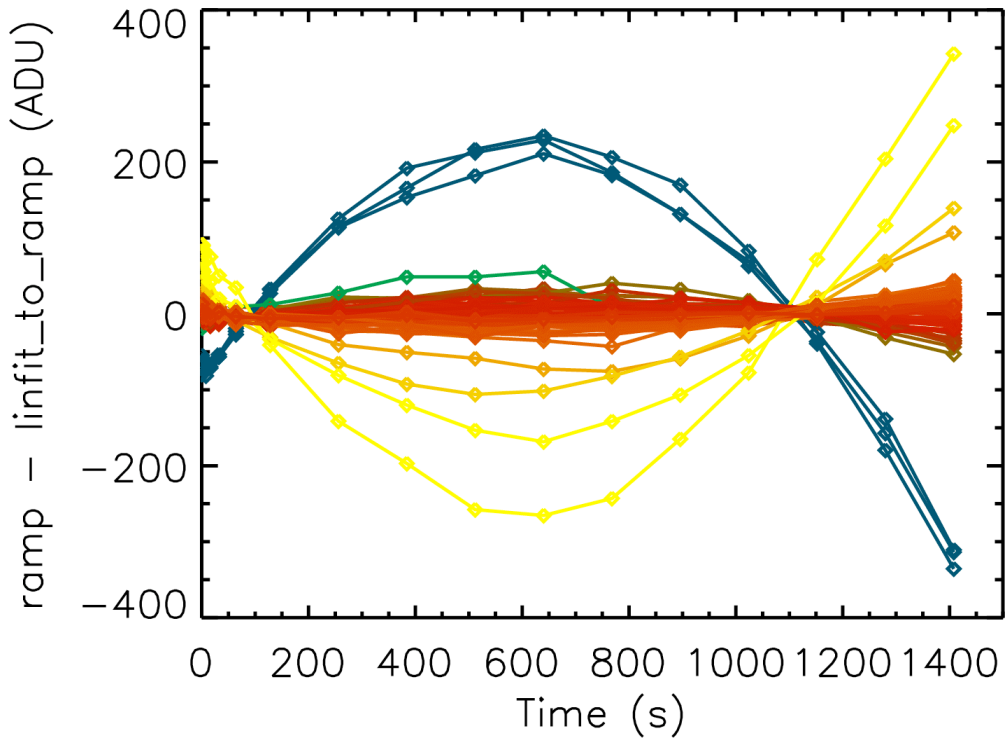


Figure 7b: Response of individual pixels relative to a straight-line fit for 64 (8x8) pixels around the point source shown in the left panel of Figure 7a.

The behavior described appears to be due to insufficient settling time in A/D conversion while clocking, although not completely consistent with pure RC rise/fall in read direction. What adds to the puzzle is that also pixels in the slow read direction follow the same pattern, although with a weaker relation. Further characterization of this behavior is underway.

Fortunately, tests show that there seems to be no effects from this curvature on aperture photometry. This is due to the symmetry of the point source shape, which means that the undershooting on the forward side cancels the overshooting on the trailing side.

New data quality (DQ) flag

If a pixel gets flagged as having at least three CR hits, then `calnica` interprets this as being a sign of curvature and not due to multiple CRs. The initially set CR flags are thereafter reset and `calnica` fits a straight line to the up-the-ramp sampling using all reads. The pixel that was affected by curvature will be flagged in the DQ extension of the `_cal` file as follows:

Flag Value: 16384

Bit Setting: 0100 0000 0000 0000

Flag Meaning: Curvature in detector response

Check for _spt file

Calnica has the option to calculate temperature dependent dark files from the reference file given by the TEMPFIL keyword. The temperature is read from the mounting cup sensor and is given by the NDWTMP11 keyword in the *_spt* file accompanying the *_raw* file. In the previous version, the temperature was set to zero if the *_spt* file was missing, which would have led to an erroneous calculation of the temperature dependent dark file. However, as of writing this, the temperature dependence of the dark files has not been implemented yet so there have been no effects of these zero temperatures. However, as a precaution against possible future use of the NDWTMP11 temperature, calnica now checks if the *_spt* file is present, and if it is not, the program exits with a message “*Error accessing _spt file*”.

Spike Rejection Update

A spike is characterized by an elevated signal affecting only a single read during the sampling (contrary to the signal of a CR which affects all reads following the CR hit). A spike is therefore detected as an elevated signal in one read, followed by a drop of the same order in the following read. A bug in the previous version of calnica did, however, under some circumstances misidentify spikes and flag them as CRs, which led to a faulty calculation of the count rate. This has now been fixed.

A further complication is the detection of a spike affecting the first read of the sample. This case does not show the characteristic rise then fall feature of the spike, instead there is only a drop between the first and the second read. The algorithm used to detect a spike checks if the first-read outlier is some threshold larger than the second-read outlier. However, this is highly susceptible to false positives if there is a CR later on in the sequence. By applying this test after the CR rejection has been done, the new version of calnica is not affected by these false positives.

Saturation in Zeroth Read

Even in the case of a moderate number of counts, some pixels may mistakenly be flagged as being saturated in the zeroth and first reads. This is a result of a faulty nonlinearity correction reference file (NLINFILE). This file has some grot-affected pixels with very low saturation values. The zero-signal correction estimates the flux in the zeroth read and flags the pixel as being saturated in the zeroth read if the value is greater than the saturation value given in the reference file. The output value for these pixels will be set to zero, since there are no unsaturated reads in the sample. This effect is largest for NIC1, with ~ 24 affected pixels, while NIC2 and NIC3 have ~ 3 and ~ 6 affected pixels, respectively, somewhat dependent on flux level.

To correct this, the saturation values in the nonlinearity reference file were made to be greater than 15,000 for all grot affected pixels. These new reference files will be distributed to CDBS.

The File Extensions of the NICMOS *_cal* files

The calibrated NICMOS *_cal* files consist of a stack of five different extensions: the science data in the SCI extension, information about errors in the ERR extension, the data quality given in the DQ extension, the number of reads in the SAMP extension, and finally, the exposure time given in the TIME extension. To complement the above description of how the SCI extension is derived, we here give a short summary of the content of the remaining extensions.

The ERR Extension

The errors assigned to the error map in the cal files produced by `calnica` consist of the uncertainty in the fit of the up-the-ramp sampling in each individual pixel. The error will therefore include the effects of read-noise, but will not include Poisson errors since these are not included in the up-the-ramp fit.

It is, however, possible for the user to add the Poisson contribution by hand. To do this, add in quadrature the Poisson contribution to the errors already in the ERR extension. In the default case, where the count rate in the SCI extension is normalized to counts/s, the Poisson contribution will be: $\sqrt{\text{SCI}/(g*\text{TIME})}$, where the exposure time is given by the TIME extension and g is the detector gain (given by header keyword `ADCGAIN`). Since the errors in the ERR extension represent the read noise, the total error including both Poissonian and read noise contributions can be calculated as

$$\text{ERR}(\text{total}) = \sqrt{\text{SCI}/(g*\text{TIME}) + \text{ERR}^2}$$

The DQ Extension

The data quality extension contains flags from the bad pixel mask (given by header keyword `MASKFILE`) in combination with flags set by the calibration performed by `calnica` (e.g., saturation, curvature in response). Compared to the previous version of `calnica`, the new flag 16384 “Curvature in detector response” is added as described above.

The SAMP Extension

The SAMP extension includes information on how many of the reads were used when calculating the up-the-ramp slope. This number can be smaller than the actual number of reads during the exposure due to e.g., cosmic rays and saturation.

The TIME Extension

TIME extension gives the exposure time used to calculate the up-the-ramp slope, and as with the SAMP extension, excluded are intervals not used due to cosmic rays and saturation. Compared to the previous version of `calnica`, this version does not include the zeroth read (0.3s) when calculating the slope.

Testing of `calnica` during implementation of updates

List of Observations

In order to test the numerous new algorithms that were implemented in this update to `calnica`, we used a number of test datasets to investigate whether or not the new `calnica` algorithm was performing as expected.

We used a set of calibration darks with a variety of `SAMP_SEQ` and `NSAMP` combinations to investigate the low S/N regime. Using a variety of `NSAMPs` allowed us to test the up-the-ramp fitting algorithm on both a large and small number of reads, as well as with a varying number of CR hits. Furthermore, we also made sure to select both linear sampled `STEP Sequences`, as well as logarithmically scaled `SPARS sequences`. For the high S/N regime, we used calibration flat-field images from a variety of filters with different exposure times. This allowed us to check different S/N levels, and thus testing to make sure that varying S/N would not affect the outcome of the new `calnica` algorithm.

In order to be sure that there would be no problem using the new `calnica` algorithm to process old datasets, we made sure to test an equal amount of datasets that were taken before and after the installation of the NCS in 2002. Even though the changes to the `calnica` algorithm should only effect `MULTIACCUM` images run through `calnica`, we also used an all `ACCUM` dataset to be sure that it could still be processed with `calnica` without causing any failure. These test datasets were selected from calibration exposures that were not dithered. This allowed us to perform statistical tests on a pixel-by-pixel basis. We also included two datasets consisting of science images, i.e., observations of standard stars and a crowded stellar field. The list of observations and dataset names used in this testing are listed in Table 2.

Camera	Image Type	Filter	Pre or Post NCS	# of Exposures	Program ID	Multiaccum or Accum	Samp_seq/Nsamp
High S/N Test Cases							
NIC1	Flat	F110W	Post	40	n9vo	Multiaccum	
NIC1	Flat	F145M	Pre	18	n43k	Multiaccum	
NIC2	Flat	F110W	Pre	19	n3wo	Multiaccum	
NIC2	Flat	F160W	Post	15	n9jj	Multiaccum	
NIC2	Flat	F207M	Pre	9	n43k	Multiaccum	
NIC3	Flat	F108N	Pre	19	n3wo	Multiaccum	
NIC3	Flat	F160W	Post	12	n6ku	Multiaccum	
NIC3	Flat	F160W	Pre	12	n43k	Multiaccum	
Low S/N Test Cases							
NIC1	Dark	Blank	Pre	85	n45z	Multiaccum	Step32/17
NIC1	Dark	Blank	Post	16	n48u	Multiaccum	Step64/26
NIC2	Dark	Blank	Pre	12	n4c1	Multiaccum	Spars256/10
NIC2	Dark	Blank	Post	17	n9jj	Multiaccum	Step128/11
NIC3	Dark	Blank	Pre	35	n8ax	Multiaccum	Spars64/13
NIC3	Dark	Blank	Post	50	n8t4	Multiaccum	Step256/13
NIC3	Dark	Blank	Post	22	n626	Accum	
Special Test Cases							
NIC2	Science	F110W	Post	74	n8q6	Multiaccum	
NIC1	Standard Star	F190N	Post	52	n8hl	Multiaccum	

Table 2: List of datasets used in testing the new `calnica` algorithm.

Testing Methods

Both the raw and calibrated images for each of these datasets were retrieved from the HST archive OTFR system. The calibrated data (using `calnica` version 4.1.1 of 14 Aug 2002) were used as a comparison to determine improvements in the new version of `calnica`. For each update in the `calnica` code, new `_cal` files were created from the original de-archived `_raw` files. A simple diagnostics script was run to determine if the code ran without failure, meaning that a correct number of `_cal` files were created in the `calnica` processing. Each run also produced some basic statistics of the test set, which were examined to determine the quantitative improvement in the S/N of the newly processed datasets. These simple statistics included the mean, min and max of the standard deviation of the old `calnica _cal` file subtracted by the newly created `calnica _cal` file. These statistics continually improved each time a new fix was made to the `calnica` code. We also checked all of the additional extensions produced by `calnica` to make sure that there were no unexpected changes to any of the non-science extensions.

Using this extensive testing, a number of unexpected bugs in the code were revealed and were fixed. For example, running a test version of the `calnica` on NIC2 using the science case images led to repeat failures until it was found that the curvature in the detector response triggered the CR detection and the hard coded maximum number of

allowed CR hits per exposure was exceeded. This anomaly was fixed in the final `calnica` code, as described above (page 9), and the `calnica` code no longer failed due to the cosmic ray limit being exceeded.

Final testing

As a final comprehensive test, we run the new final `calnica` version on four extended data sets in order to verify the behavior and quantify the improvements in `calnica`. Again, these include both low and high S/N observations as well as science data.

Flat-fields – Analysis of High S/N Case

The new `calnica` was run on the full set of flat-field images obtained during the NICMOS calibration program 11016 (P.I: N. Pirzkal). This includes flat-fields for all available combinations of cameras and filters/grisms/polarizers, in total 57 different flat-fields. To get a quantitative estimate of the improved behavior of the new `calnica`, we estimate the S/N in each flat-field using both the old and the new `calnica` versions. For each pixel, we calculate the rms around the mean for the 8 images (typical number) that are combined to produce the flat-field. The S/N in each pixel is then given by the value of the flat-field divided by the rms. For each flat-field, we then assign a S/N value that is the median of the S/N values of the individual pixels. Finally, to quantify the change in S/N, we divide for each flat-field median the S/N produced by the new `calnica` with the value from the old version. In Figure 8, we show the distribution of relative S/N values. It is reassuring that all 57 flat-fields show an increase in S/N. The median increase in S/N is $\sim 6\%$ (mean increase $\sim 9\%$).

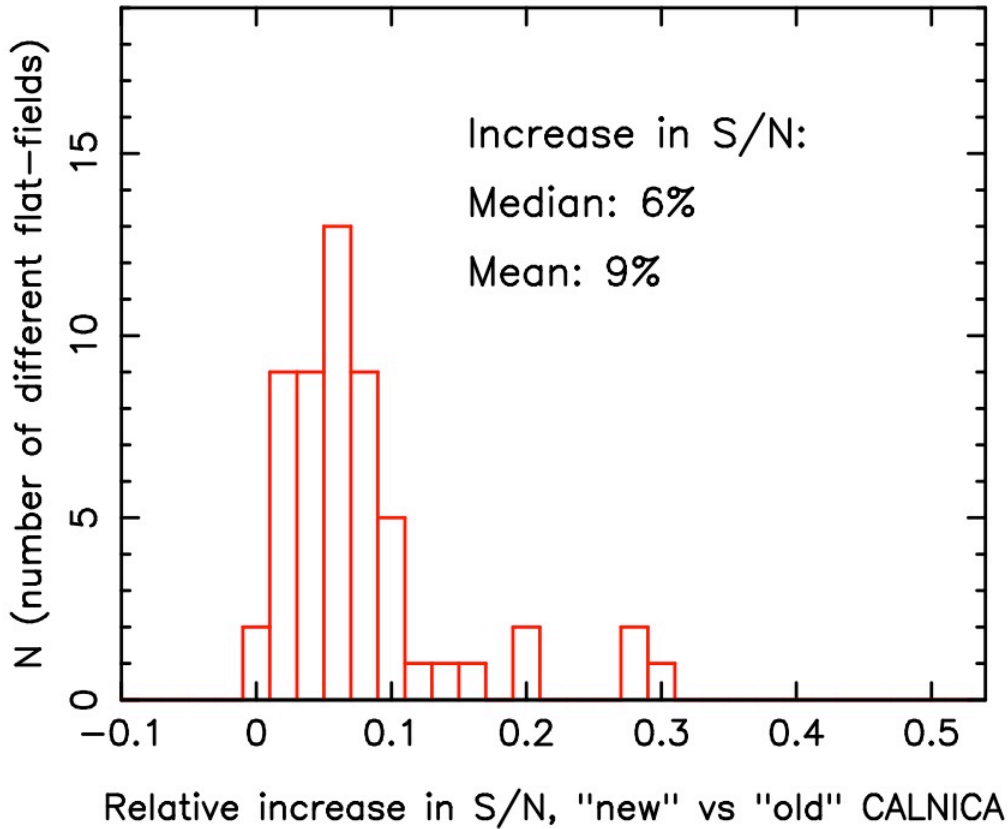


Figure 8: Relative increase in Signal-to-Noise when using the new `calnica` as compared to the old version of `calnica`. Results are shown for a set of 57 flat-field images. Median increase in S/N is ~6%.

Darks – Analysis of Low S/N Case

To investigate the low S/N regime, we use a set of 290 dark images obtained during the NICMOS dark monitoring calibration programs 2002-2008. All images used were taken with the SPARS64 sequence and with NSAMP=20, giving each image an exposure time of 1088s. After calibrating these images using both the old and the new versions of `calnica`, we combine the images and calculate the S/N in each pixel as described in the previous section. The difference in S/N between the old and new `calnica` is marginal, with an increase of S/N of ~1% (in both median and mean) when using the new version. This small difference is expected since the difference in the weighting of the up-the-ramp sampling is the smallest in the low S/N regime.

Standard Stars – Analysis of Impact to Photometry

The new `calnica` routines were checked with all the photometric observations used for deriving the photometric zeropoint of NICMOS. After the `calnica` data reduction and the standard further photometric pipeline reduction the error in the calibration data is dominated by the change of temperature over time, slowly reducing the sensitivity. Taking this trend out with the temp-from-bias routine under development by the

NICMOS team there are still some systematic deviations remaining. Therefore, even though the RMS is less than 1% in the best filter/camera combinations, the improvement in S/N over all observations is small (typically about 1%). However, this test does show that the new `calnica` is robust and gives at least as good results as the old `calnica` for more than 20,000 photometric observations.

Grisms observations

The new `calnica` was tested with NIC3 grism observations for four different stars and a total of seven different data sets. These observations include one bright star HD165459 (data sets na5311, na5312), a middle brightness WD star G191B2B (n9u201, n9u204), and two faint stars WD1657+343 (n8vj03, n9u208) and Snap-1 (n9u218). Data sets included all three grisms G096, G141, and G206, except for WD1657+343, which is too faint for G206 spectra.

New `calnica` spectra extracted from the new `_cal.fits` images with a height of four pixels are compared with the same extractions for the original data processing. The only differences between the spectra are the new `calnica _cal.fits` files. Subsequent processing is identical, including the same original flat fields.

Any systematic change due to the new processing is less than 1%. Pixel-to-pixel changes increase from $< \sim 0.1\%$ for the bright star HD165459 up to the occasional difference of $\sim 2\%$ for G141 observations of WD167+343. Small `calnica` differences in the `_cal.fits` images are magnified when comparing the NET spectra that are tiny signals on top of large backgrounds. In the worst case of G206 for Snap-1, where the signals are just a percent or so above the typical spectral background of ~ 300 DN/s, differences in the NET are often more than 5% for individual sample points.

Summary and Conclusions

We have here presented a number of updates to `calnica`, the task that performs instrumental calibration of NICMOS data. The two major improvements concern the way reads are weighted when determining the count rate from the up-the-ramp-fitting and the way cosmic rays are corrected for. Besides these, we have also described a number of minor updates. With the new way of calculating count rates, the error extension in the calibrated NICMOS images now has a more physical interpretation, representing the read-noise. Extensive testing shows an expected decrease in scatter of 6-15% using the new `calnica` in the high S/N regime. The difference is expected to be smaller at lower S/N.

The new `calnica` will have version number `calnica 4.2` and will be implemented in the upcoming STSDAS release (second half of 2008), and will be in the next OPUS release (2008.2).

References

- Fixen, D. J., et al. 2000, PASP, 112, 1350
- Regan, M., 2007, JWST-STScI-001212